Iranica Journal of Energy and Environment
Journal Homepage: www.ijee.net
IJEE an official peer review journal of Babol Noshirvani University of Technology, ISSN:2079-2115

Effect of Diesel-engine Operating Conditions on Performance of Waste Heat Recovery Cycles: A 4E Analysis

B. Alizadeh Kharkeshi, R. Shafaghat*, S. Talesh Amiri, A. M. Tahan, A. Ardebilipour

Faculty of Mechanical Engineering, Sea-Based Energy Research Group, Babol Noshirvani University of Technology, Babol, Iran

P A P E R I N F O

Paper history:
Received 04 August 2023
Accepted in revised form 02 October 2023

Keywords:
Experimental study
Fuel energy saving ratio
HD diesel engine
Waste heat recovery

A B S T R A C T

In waste heat recovery from a heavy-duty diesel engine, with a focus on engine speed's impact, is explored. The critical problem of enhancing energy efficiency and reducing emissions through waste heat utilization is addressed. Waste heat in internal combustion engines, vital for sustainable energy use and environmental preservation, is investigated. Experimental analysis and thermodynamic modeling introduce Organic Rankine Cycle (ORC), Steam Rankine Cycle (SRC), and Combined Steam and Organic Rankine Cycle (CSO) for waste heat recovery. A non-linear relationship between engine speed and waste heat is identified. Waste heat increases up to 1600 rpm and decreases thereafter. The CSO cycle outperforms ORC and SRC cycles, achieving 43.4% higher efficiency. Fuel energy savings demonstrate CSO's superior economy, along with excellence in Annual Carbon Dioxide Emissions Reduction (ACO2ER). Waste heat recovery knowledge is advanced by introducing the efficient CSO cycle, contributing significantly to existing research.

***Doi**: 10.5829/ijee.2024.15.03.01*

INTRODUCTION

Due to the increase in population and the development of industries, the rate of fossil fuels consumptions has significantly inceased. In this regard, various heat recovery cycles are used for the best utilization of fossil fuel sources (such as CHP, CCHP, ORC, SRC and CSR). Depending on the prime mover, different recovery cycles, such as thermoelectric, phase change materials, and ORC, can be selected. If the application requires power generation, heat recovery cycles that can generate power are appropriate, and these cycles mainly include ORC, SRC, and CSR by energy and exergy analysis (1). Extensive studies have been presented for using waste heat of various types of prime movers. The following studies can be mentioned.

In 1981, Brands et al. (2) investigated the waste heat recovery of a 14.5-liter six-cylinder NTC-400 type diesel engine with a power of 298 kW; they showed that the waste heat recovery of a diesel engine using the Rankine cycle can increase engine power by 12.5% (at 2100 rpm). In 1983, DiBella et al. (3) showed that using the ORC cycle to recover the waste heat of the engine with TFL fuel with a power of 288 hp could lead to a better engine performance in road tests also, using the ORC cycle increased the efficiency by 12.5% in the road test. In 2007, Endo et al. (4) investigated maximizing exergy efficiency in car engines; design changes, including the cylinder head and cooling passages, were made to the base 2-liter Honda Stream SI engine to maximize exhaust energy recovery and lead to improving thermal efficiency by 13.2%.

In 2011, He et al. (5) investigated an ORC thermodynamic cycle for engine waste heat recovery. They showed that exhaust gas, cooling, and lubricating water could be a suitable source of heat supply for the heat recovery cycle. Moreover, they proposed an ORC and SRC thermodynamic cycle for engine waste heat recovery. Shu et al. (6) in 2013 simulated an ORC cycle to recover the waste heat of a diesel engine. By experimentally measuring the recoverable heat of the engine and investigating the effect of using the recovery cycle on performance, they showed that the ORC cycle could produce 18.8 kW or 9.6% power for the engine. In 2014 Jalili et al. (7) introduced the application of

*Corresponding Author Email: rshafaghat@nit.ac.ir (R. Shafaghat)

Please cite this article as: Alizadeh Kharkeshi B, Shafaghat R, Talesh Amiri S, Tahan A. M., Ardebilipour A. Effect of diesel-engine operating conditions on performance of waste heat recovery cycles: A 4E analysis, Iranica Journal of Energy and Environment, 2024 July, 15(3): 220-34. Doi: 10.5829/ijee.2024.15.03.01

nanotechnology in air conditioning systems to improve efficiency. The experimental study involves using water-nanoparticle mixtures, particularly carbon nanotubes (CNTs), in a refrigeration cycle. Results show that increasing CNT concentration leads to significant temperature gradients, highlighting the potential of nanoparticles for enhancing heat transfer in refrigeration systems.

Also, Shu et al. (8) in 2016 conducted a thermodynamic evaluation of an ORC system for diesel engine waste heat recovery; the results showed that the highest energy and exergy efficiencies are 11.3% and 38.7%, respectively. The highest efficiency improvement compared to the base engine ws 16%. In 2019, Lion et al. (9) applied the thermodynamic analysis of waste heat recovery using the ORC in a marine diesel engine. The results showed that the ORC cycle implementation for waste heat recovery could reduce engine fuel consumption by 5%. In 2020, Mohammad et al. (10) investigated the use of waste heat in the ORC cycle and its effect on engine and cycle performance. They stated that the marine diesel engine is widely used in commercial ships as a propulsion system. The use of waste heat of the engines is crucial by considering the current conditions; the results showed that the heat recovery cycle could reduce fuel consumption by 18%.

In 2021, Bodaghi et al. (11) studied the waste heat recovery of a heavy diesel engine; the results showed that the operating conditions of the engine (engine speed) are essential for the performance and in the best operating conditions of the engine system, it has a thermal efficiency of 9.5% and an exergy efficiency of 43% and also the maximum exergy destruction rate of 500 kW was obtained. In 2021, Neto et al. (12) investigated the heat recovery cycle's effect on engine performance and showed that the average increase in exergy performance is 9.35%. It was also stated that using the recovery cycle leads to a reduction in fuel consumption and pollutants. In 2022, Ping et al. (13) investigated the effect of using the ORC waste heat recovery system for the engine from the energy and economic point of view. The results showed that the ORC system is used to recover the waste heat of the internal combustion engine. The change in the engine's operating conditions has effect on the recovery cycle performance. The performance of the ORC system is improved by changing the engine's operating conditions from 9.25 to 17.72%. In 2022, Luo et al. (14) conducted a comparative study between different cycle arrangements for recovering waste heat from ships' diesel engines. They showed that the ORC system for waste heat recovery can increase power up to 49.83 kilowatts.

Using the waste heat of internal combustion engines (especially HD diesel engines) is one of the best ways to increase the efficiency of this type of prime mover. In this regard, the review of previous studies showed (to the authors' best knowledge) that a thermodynamic research should be applied for each specific engine separately to determine the proper selection of the heat recovery cycle. in this regard, in this research, the MTU 4000 R43L HD diesel engine heat recovery potential was evaluated by experimental measurements technique and the help of thermodynamic equations. The thermodynamic modeling was applied to model an ORC, SRC, and CSO by considering critical technical constraints related to back pressure and dew point for waste heat recovery. In order to further investigate the effect of engine speed (as a crucial parameter) on the waste heat has been studied, the waste heat for three sources of the intercooler, water heat exchanger, and exhaust gas heat has supplied three ORC, SRC, and CSO cycles for waste heat recovery. Engine waste heat was modeled from the energy and exergy point of view. Also, to achieve an accurate comparison from an economic perspective, the new system with waste heat recovery was compared with conventional power generation systems, so the fuel energy saving ratio (FESR) was also investigated, The advantages of this study is as follows:

1. Comprehensive evaluation: 4E analysis covers economic, environmental, energy, and exergy aspects, providing a well-rounded assessment of waste heat recovery systems.
2. Practical relevance: Focusing on heavy-duty diesel engines makes research directly applicable to industries where these engines are prevalent.
3. Economic viability: Demonstrating the cost-effectiveness of the Combined Steam and Organic Rankine Cycle (CSO) compared to other cycles attracts industry stakeholders.
4. Environmental impact: study's environmental analysis highlights the CSO cycle's potential to reduce carbon dioxide emissions, aligning with sustainability goals.
5. Exergy efficiency: The inclusion of exergy analysis helps identify sources of inefficiency, showcasing the CSO cycle's ability to capture and utilize waste heat effectively.
6. Contributing to Research: Introducing the CSO cycle advances waste heat recovery knowledge and benefits researchers and practitioners in the field.

MATERIALS AND METHODS

Prime mover (HD diesel engine)

The MTU 4000 R43L engine is a 16-cylinder internal combustion HD diesel engine used in transport applications. Due to the increase in the temperature of the air coming out of the turbocharger, an intercooler is used to cool the air entering the cylinders. The detailed specifications of this engine are presented in Table 1. Also, Figure 1 shows the schematic arrangement of the

cylinders and the air path in the engine block.

A common rail system injects fuel directly into the combustion chamber in this engine. Table 2 shows the specifications of the direct and port fuel injection system. Also, diesel fuel specifications are presented in Table 3.

The performance of the MTU4000 R43L engine was studied in an experimental test. Figure 2 shows the schematic diagram of the engine and other equipment needed in the experimental test room.

According to the objectives of the present study, experimental tests have been performed. To apply the defined load, the HORIBA hydraulic dynamometer model DT3600-2 is used (Table 4). Also, the pressure inside the cylinder is measured with the help of a KISTLER 6613CA piezoelectric pressure sensor and a KISTLER 5018 amplifier.

According to the purpose and sensitivity of the problem, the temperature data of the engine and the cooling system are needed to check the feasibility of heat

Table 1. MTU 4000 R43L HD diesel engine characteristics

Parameters	Value
Number of cylinders	16V
Power	UIC 2400 kW
Engine rated speed	1800 RPM
Configuration	90°V
Bore/stroke	170/210 mm (6.7/8.3 in)
Cylinder displacement volume	4.77 l (291 cu in)
Total displacement volume	76.3 l (4656 cu in)
Compression ratio	18
Fuel properties	DIN EN 590
Intake valve closing (CAD aBDC)	5
Exhaust valve opening (CAD bBDC)	50

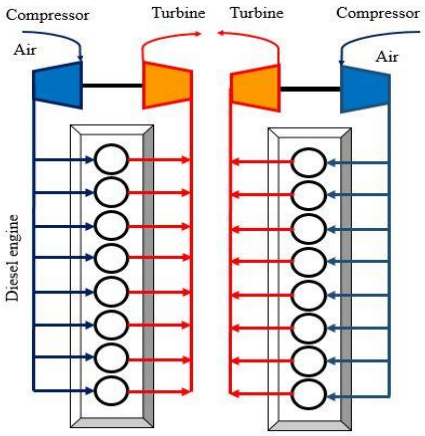

Figure 1. Schematic diagram of MTU 4000 R43L

Table 2. Specifications of direct fuel injection and port fuel injection system (15)

Items	Common-rail injection system
Number of holes	8
Hole diameter (mm)	3.5
Spray angle	6
Injection pressure (bar)	1600

Table 3. Diesel fuel specifications

Items	Diesel
Chemical formula	C12-C25
Cetane number	52.1
Octane number	-
Density (gr/mL)	0.845
Low Heating Value (Mj/kg)	42.8
Latent heat of vaporization (kJ/kg)	301
Viscosity (Mpa.s)	3.995

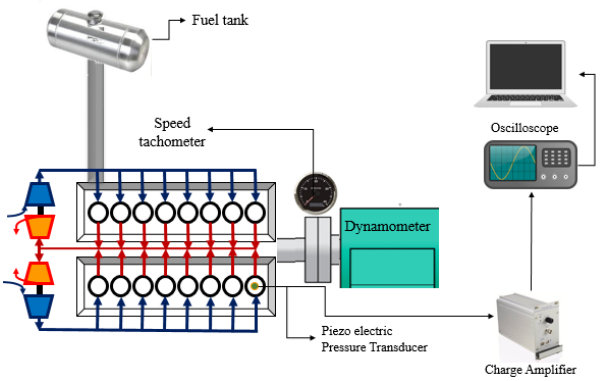

Figure 2. Schematic diagram of engine test facilities

Table 4. Specifications of HORIBA DT3600-2 hydraulic dynamometer

Item	Unit	Specification
Pnom	kW	3600
Maximal Speed nmax	1/min	3000
Rated Torque Mnom	Nm	30000
max. Share of Coupling Mass at nmax /Distance from the coupling flange	kg	280/114
Θ Rotor	kgm^2	18.4
Torsion-spring constant up to middle of the dynamometer	106 Nm/rad	11.9
Weight	kg	3200

Table 5. Laboratory measuring instruments

Measuring instruments	Type
Fuel flow meter	RHEONIK model RHM06
Back pressure sensor	PTX510- DRUCK
Temperature sensor	PT100
Fuel Pressure sensor	IFM PI28xx

recovery. Also, to check the limits of reducing the exhaust temperature in order to recover the heat, the data of the back pressure of the exhaust system should be carefully checked. For this purpose, a set of laboratory measuring instruments was used, which is introduced in Table 5.

Calculation of the thermal capacity of the target engine based on the experimental results

Temperature limits for exhaust gas include dew point temperature and back pressure limits. If the exhaust gas temperature is lower than the dew point temperature, the water droplets formed in the exhaust path will cause corrosion of the conductor. If the exhaust back pressure value exceeds the standard limit, the engine performance will be weakened.

Dew point temperature limit

To evaluate the exhaust gas temperature reduction variations based on the dew point, the values of the exhaust gas pressure at the exhaust outlet are used as the standard pressure to determine the dew point.

Dew point temperature constraint is more critical in low exhaust gas pressures where the back pressure issue is unimportant.

Exhaust gas back pressure limit

Exhaust gas is one of the main sources of heat loss. So, pressure is the most critical limitation that affects heat extraction from the exhaust gas. An excessive increase in return gas pressure causes an increase in fuel consumption and decreases the engine's thermal efficiency. Equation 1 is used to calculate back pressure.

Table 6. Calculation of dew point temperature in different engine revolutions per minute

Engine speed (rpm)	Outlet gas pressure at the turbocharger (kPa)	Dew point (ºC)
600	100.041	28.97
800	100.163	28.99
1180	100.604	29.06
1500	101.547	29.23
1600	102.186	29.33
1800	102.949	29.46

Table 7. Recommended return pressure (16)

Engine Size	Back pressure constraint
Power up to 50 kW	40 kPa
Power between 50 to 500 kW	20 kPa
Power more than 500 kW	10 kPa

$$P = (L \times \rho \times Q^2 \times 3.6 \times 10^6)/d^5 \quad [1]$$

P= Back pressure, kPa
L= Length of pipe in motor, m
ρ= Density of gas, kg/m^3
d= Diameter of pipe, m

Based on the study of Mayer (16), the back pressure limit based on engine power is presented in Table 5.

In the following, the back pressure values in different rpm are calculated based on the output pressure from the turbocharger. Based on this, the permissible temperature of the exhaust gas coming out of the turbocharger is presented in Table 6. In the cycles where the back pressure has not entered the illegal limit, the dew point temperature is considered the minimum permissible temperature of the exhaust gas.

To ensure that the exhaust back pressure is correct, the results obtained from the calculation code related to the exhaust back pressure are compared with the laboratory values, and the validation result is shown in Figure 3.

The thermal capacity of different parts of the engine according to the experimental test process in various operational modes is presented in Table 9.

Heat recovery cycle

According to previous section's investigations, three waste heat recovery cycles SRC, ORC and CSR were presented to recover the waste heat of the MTU 4000 R43L engine and were subjected to thermodynamic

Table 8. Permissible temperature of the exhaust gas exiting the converter based on back pressure

Engine speed (rpm)	Gas pressure at the turbocharger outlet (kPa)	The minimum permissible temperature of the exhaust gas leaving the heat exchanger (°C)
600	100.041	29.01
800	100.163	29.12
1180	100.604	29.71
1500	101.547	74
1600	102.186	150
1800	102.949	192

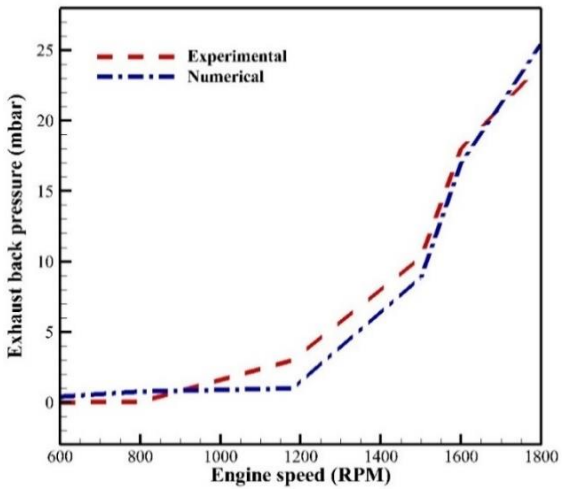

Figure 3. Validation of computational code for exhaust back pressure

Steam Rankine Cycle (SRC)

In the steam Rankine cycle (Figure 4), first, the working fluid in the evaporator receives the waste heat caused by the cooling water and the exhaust gas in two separate converters. Then it enters the turbine and performs work, then it is cooled in a process in the condenser and The initial temperature returns, and finally, the fluid is pumped to the evaporator. Assumptions have been considered in the design of the steam Rankine cycle, which will be discussed further.

Assumptions:

- The pressure of the working fluid when passing through the evaporator and condenser is constant and equal to 1000 and 10 kPa, respectively.
- The temperature of the working fluid while passing through the pump is constant and equal to 40 ℃.
- The flow rate of the working fluid is calculated according to the heat loss specific to each cycle.
- Thermodynamic efficiency of the turbine and pump is assumed to be 85%.

Table 9. Different parts of the engine in different performance conditions in the factory test

Power (kW)	Speed (rpm)	Exhaust gas	Water-Water cooler	Intercooler	Total waste heat
35	600	49	104	1.5	155
537	800	119	210	1.5	331
1200	1180	365	415	2.0	782
1900	1500	593	529	1.3	1123
2250	1600	708	845	3.2	1556
2540	1800	553	950	4.0	1506

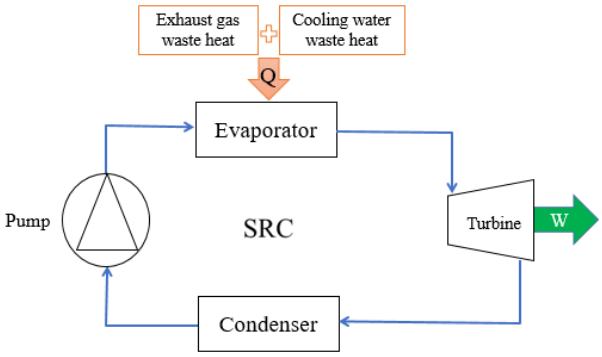

Figure 4. Schematic diagram of steam Rankine cycle

The heat of the engine cooling system is used to preheat the working fluid, and the exhaust gas waste heat is used to bring the fluid to the condition of superheated steam.

Organic Rankine Cycle (ORC)

The organic Rankine cycle works like the steam Rankine cycle. With the difference that the operating fluid in this cycle is an organic fluid. Other differences are in the assumptions section. The working fluid in this cycle is R134fa. The relations governing this cycle are the same as the Rankine steam cycle.

Assumptions:

- The temperature of the working fluid at the beginning and end of the evaporator is assumed to be constant and equal to 25℃ and 80℃.
- The temperature of the working fluid when passing through the pump (compressor) is constant and equal to 25℃.
- The flow rate of the working fluid is calculated according to the heat loss specific to each cycle.
- Thermodynamic efficiency of the turbine and pump is assumed to be 85%.
- Condenser and turbine are assumed to have constant entropy.

The schematic diagram ORC cycle is shown in Figure 5.

Combined organic and steam Rankine cycle (CSO)

In the combined cycle (Figure 6), the exhaust gas heat is used for the SRC, and the engine cooling system's heat is used to preheat the ORC. In the combined cycle, two separate circuits will operate from each other. Due to the difference in the nature of the two working fluids, two different turbines, pumps, and condensers are required in the combined cycle. The relationships governing this cycle are the same as the previous two cycles.

Assumptions of the organic Rankine cycle in the combined cycle:

- The temperature of the working fluid at the exit from the condenser and when passing through the compressor (pump) is assumed to be constant and equal to 25℃.

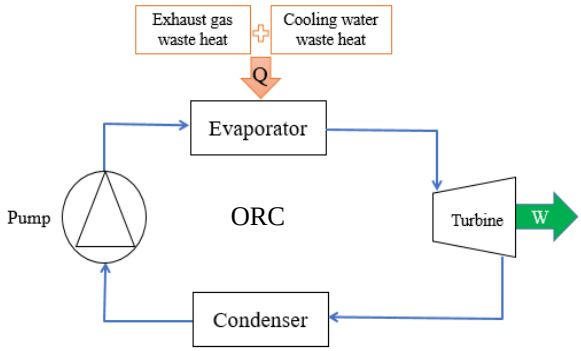

Figure 5. Schematic diagram ORC cycle

– The working fluid pressure is assumed to be constant while passing through the evaporator and condenser.
– Thermodynamic efficiency of turbine and compressor is assumed to be 85%.

Assumptions of steam Rankine cycle in combined cycle:

– The temperature of the working fluid at the exit from the condenser and when passing through the pump is assumed to be constant and equal to 40°C.
– The working fluid pressure is assumed to be constant while passing through the evaporator and condenser.
– Thermodynamic efficiency of the turbine and pump is assumed to be 85%.

It should be noted that the work of the combined cycle is obtained from the sum of the work in the organic Rankine and steam Rankine cycles.

Thermodynamic modeling

Law of conservation of mass and energy

In the steady state for a specific control volume, the energy and mass equations are as follows:

$$\sum \dot{m}_e - \sum \dot{m}_i = 0 \qquad [2]$$

$$\dot{Q} + \sum \dot{m}_i\, h_i = \dot{W} + \sum \dot{m}_e\, h_e \qquad [3]$$

where h is the specific enthalpy, fuel energy is calculated using Equation 3 (15, 17).

$$\dot{Q}_{fuel} = \dot{m}_{fuel} LHV \qquad [4]$$

In Equation 4, the LHV is the fuel's low heating value. system's efficiency from the energy viewpoint of the system is calculated according to Equation 5.

$$\eta_{th} = \frac{\text{total energy output}}{\text{total energy input}} \qquad [5]$$

Exergy analysis

Exergy equations for a control volume are as follows (18):

$$\dot{E}x_Q + \sum \dot{m}_i ex_i = \dot{E}x_w + \sum \dot{m}_e ex_e + \dot{E}x_D \qquad [6]$$

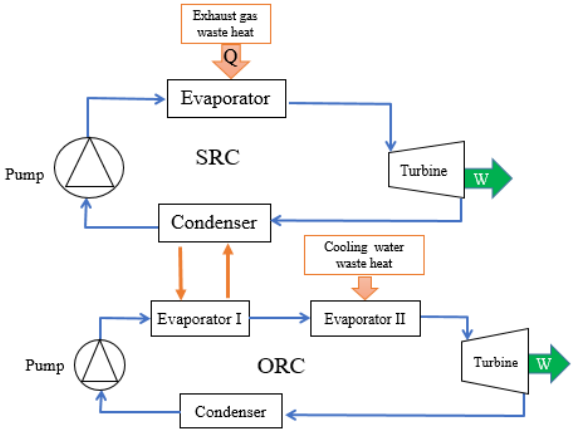

Figure 6. Combined cycle schematic

$$\dot{E}x = \dot{m}ex \qquad [7]$$

where ex and $\dot{E}x_D$ are specific exergy and exergy destruction rate, respectively. In Equations 6 and 7, $\dot{E}x_Q$ and $\dot{E}x_w$ are the exergy related to the heat transferred and the work done between the control volume and the environment (18).

$$\dot{E}x_Q = \dot{Q}\left(1 - \frac{T_0}{T}\right) \qquad [8]$$

$$\dot{E}x_w = \dot{W} \qquad [9]$$

In Equation 8, T_0 represents the ambient temperature. Specific physical exergy in a certain state is defined as follows (19):

$$ex_{ph} = (h - h_0) - T_0(s - s_0) \qquad [10]$$

Index 0 shows the value of a variable in environmental conditions. Also, the amount of chemical exergy for an ideal gas mixture is expressed by Equation 11 (19, 20).

$$ex_{ch.mix} = \left[\sum_{i=1}^{n} X_i ex_{ch_i} + RT_0 \sum_{i=1}^{n} X_i \mathrm{Ln}\,(X_i)\right] \qquad [11]$$

Fuel energy saving ratio

The FESR has been discussed in this section. For calculating this parameter, it needs to be compared recovered system to a conventional energy supply system. Fuel Saving (FS) can be defind, stated as follows (18):

$$FS = \frac{\dot{W}_{Eng} + \dot{W}_{WHR}}{\eta_{con}} - F_{Conv} \qquad [12]$$

There is an expression for calculating FESR, this term means if the consumer uses a recovered system in comparison with conventional energy systems, how much energy saving can be achieved, so this parameter can be written as follows (18):

$$FESR = \frac{\text{FS}}{\frac{\dot{W}_{Eng} + \dot{W}_{WHR}}{\eta_{con}}} \qquad [13]$$

Environmental modeling

Some of the advantageous parameters for environmental evaluations in the waste heat recovery are introduced by annual reduction in CO_2 emissions and reducing tax costs. To calculate the Annual CO_2 Emission Reduction (ACO_2ER) for the proposed system, first, CO_2 emission rates of the proposed system has been calculated as follows (21, 22):

$$mCO_2^{conv} = \mu CO_2^W \cdot P_{el} \quad [14]$$

$$mCO_2^{Hybrid} = \mu CO_2^F \left[\frac{\dot{W}_{Eng} + \dot{W_{WHR}}}{\eta_{con}}\right] \quad [15]$$

$$ACO_2ER = \frac{\left(mCO_2^{Conv} - mCO_2^{Hybrid}\right)}{10^6} \quad [16]$$

$$ACO_2TR = \left(mCO_2^{Conv} - mCO_2^{Hybrid}\right) \cdot \gamma_{CO2} \quad [17]$$

where γ_{CO2} is CO_2 tax rate, and is equal with 0.00003 \$ g^{-1} (23).

Uncertainity analysis

The dynamometer which has been used in this study is hydrolic dynamometer with the error of 0.4%. The dynamometer intervals were 1 N.m and the uncertainity anlaysis is as follows:

$$u_B = \frac{a}{\sqrt{3}} \quad [18]$$

$$u_c = \sqrt{u_B^2} \quad [19]$$

$$U = K\, u_c \quad [20]$$

u_c is the mean uncertainty, and U is the combined uncertainty with the overlap coefficient K. If K is considered equal to 2, then the assuredness level of the results can be increased to 95%. Therefore the uncertainity is 1.2 N.m. Other instrument uncertainity analysis is shown in Table 10.

RESULTS AND DISCUSSION

Recoverable heat of the primary drive

Figure 7 shows the graphical representation portrays the influence of engine speed on output power. It is readily discernible from this graphical depiction that elevating the engine speed results in a concomitant augmentation of power output. Within the range under investigation, this escalation in power exhibits a conspicuously robust and upward trajectory, underscoring the pronounced influence of engine speed on power generation.

Table 10. Uncertainity and error results

Measuring instrument	Error	Interval	Uncertainity
Fuel flow meter	±0.1 %	0.01 (lit)	0.011 (lit)
Back pressure sensor	±0.2%	0.1 (bar)	0.11 (bar)
Temperature sensor	±0.05°C	0.1 K	0.11 (K)
Fuel pressure sensor	±5%	0.1 (bar)	0.11 (bar)

Within the context of internal combustion engines, it is imperative to recognize that the energy input into the engine is not solely converted into useful work; a substantial portion is also transformed into heat. To effectively manage this thermal energy and prevent overheating, a suite of heat exchange mechanisms is employed. These heat sources encompass an intercooler, a water-cooling system, and the heat generated by exhaust gases during engine operation.

In the accompanying figure, a comprehensive analysis of the impact of engine speed on heat generation within each section is depicted. It is noteworthy that the recoverable heat in the intercooler is found to be relatively insignificant when compared to the substantial heat potential inherent in the water-cooling system and the exhaust gases emanating from the engine. This observation underscores the vital role played by the water-cooling system and exhaust heat recovery mechanisms in harnessing and utilizing thermal energy efficiently.

Furthermore, an intriguing aspect emerges when considering the behavior of the intercooler temperature with respect to engine speed. At lower engine speeds, characterized by revolutions per minute (rpm) up to 1500, the intercooler temperature remains fairly stable, experiencing minimal fluctuations. However, as engine speed surpasses the 1500 rpm threshold, a pronounced and noteworthy rise in intercooler temperature becomes evident. This temperature pattern has significant implications for the management of engine cooling and highlights the need for tailored strategies to mitigate the increase in heat.

Turning our attention to the exhaust gases, it is discernible that the maximum available heat from this source is achieved at an engine speed of 1600 rpm. Beyond this particular engine speed threshold, there is a discernible decrease in the heat generated by the exhaust gases. This insight is crucial when considering the optimization of heat recovery systems or the utilization of exhaust gas energy for other applications.

Conversely, the heat available within the water heat exchanger section exhibits a contrasting trend. It showcases a relatively linear relationship with engine speed. Remarkably, this heat source consistently amplifies as engine speed increases, offering an attractive opportunity for efficient harnessing and utilization.

In summary, the graphical representation provided offers a comprehensive view of the intricate relationship between engine speed, power output, and the distribution of heat within various engine components. These

observations are indispensable for enhancing our comprehension of engine performance characteristics, guiding the development of effective cooling and heat recovery strategies, and facilitating informed decision-making in the design and operation of internal combustion engines.

In order to achieve a comprehensive analysis of the effect of the engine speed on the total heat produced by the engine at different speeds, increasing the engine speed up to 1600 rpm leads to an increase in the available heat for recovery by cycles. It is recovered, but after passing this speed, the available heat decreases; the critical point is that in the lowest test cycle (600 rpm) the heat that can be recovered is 153.4 kW, which is a significant amount. Also, the system in the best condition (1600 rpm) has recoverable heat equal to 1600 kW, which is crucial and should be recovered. Figure 8 shows the effect of engine speed on total waste heat.

Comparison of ORC and SRC cycles

To recover the produced heat in the diesel engine, two scenarios have been predicted. in the first scenario, an ORC cycle has been proposed to generate power from the engine's waste heat, and in the second scenario, an SRC cycle has been proposed to recover the waste heat; If the waste heat of the engine enters each of these cycles and the power is produced, the results ar illustrated in Figure 9. It is clear from this diagram, in all engine revolutions per minute, the power produced by the ORC cycle is more than SRC, but with this difference that at low revolutions per minute, the performance of ORC and SRC system is very close to each other, but as the revolutions per minute increase and reach 1180 revolutions per minute, the difference between the performance of ORC cycle and SRC cycle increases and It can be said that using the ORC system for high engine speed is very vital. The system with the ORC cycle produces 3.6% more power in the best state. Also the performance of both cycles was studied, the results showed that the system has lower efficiency in low revolutions per minute compared to high engine speed; On the other hand, for all revolutions per minute, the ORC cycle has more efficiency than the SRC cycle, and the efficiency results show that up to 1180 rpm, both cycles experience an increase in efficiency with the rise of the engine speed. However, the engine speed does not significantly increase the converter's efficiency after passing this point. Also, the efficiency of the ORC cycle is 10.5% better than the SRC cycle in the worst condition, and the performance of the ORC cycle is 6.6% better than the SRC cycle in the highest point.

In the Figure 10, the effect of increasing the engine speed on the exergy destruction of two ORC and SRC cycles is shown. As it is clear from the diagram, for both cycles, the exergy destruction rises by increasing the engine speed up to 1600 rpm. But after passing the optimal point, the exergy destruction decreases slightly for both cycles. From the exergy point of view, the important point is 1600 rpm. The SRC cycle has much higher exergy destruction than the ORC cycle, so the exergy destruction of the ORC cycle is, on average, 9.8% of the SRC cycle, which shows that the ORC cycle has much less exergy destruction. The cause of this behavior

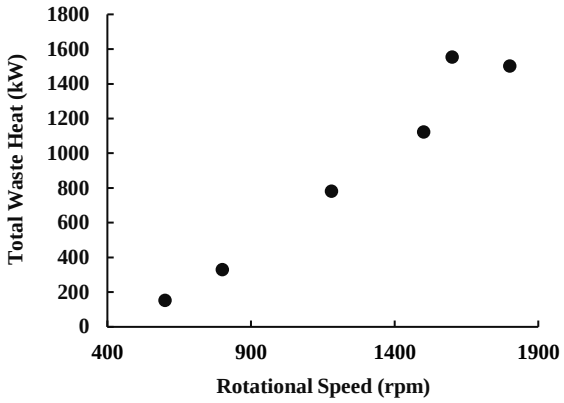

Figure 8. Effect of engine speed on total waste heat

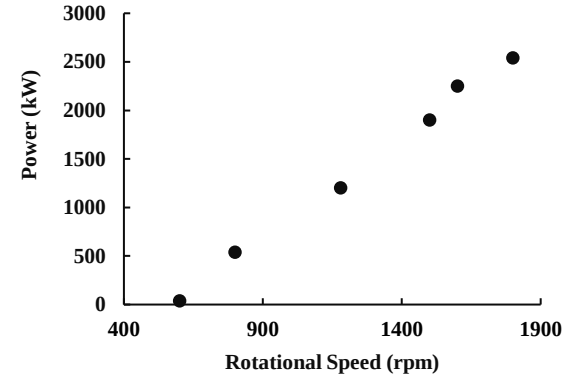

(a)

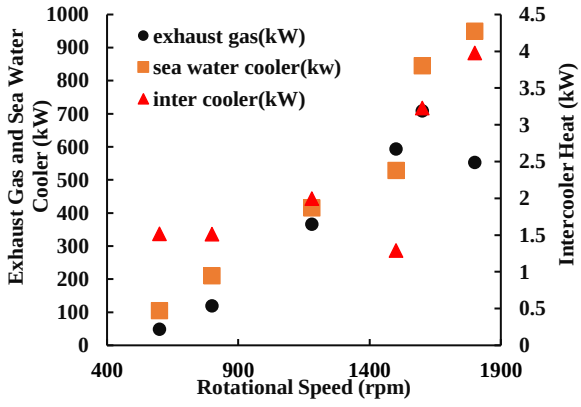

(b)

Figure 7. Effect of engine speed on (a) power, and (b) waste heat by details

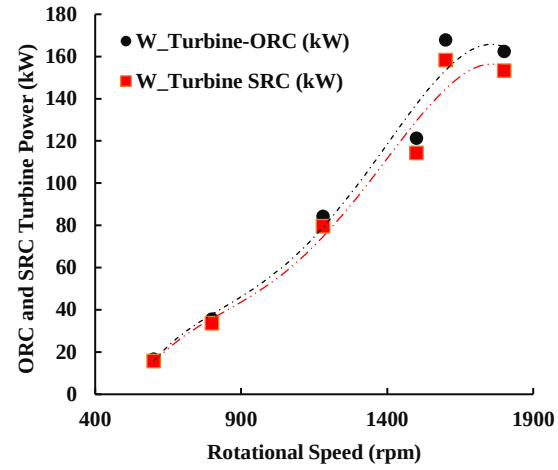

(a)

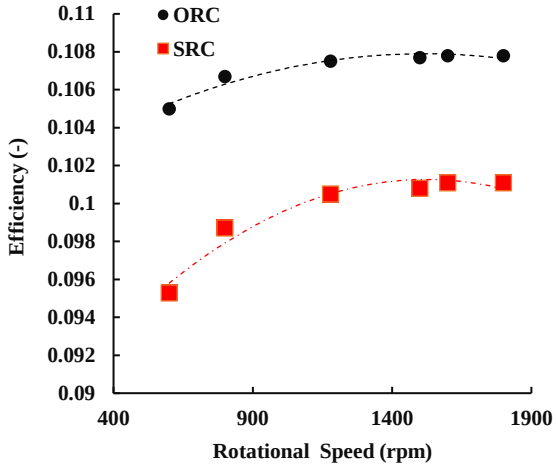

(b)

Figure 9. Effect of engine speed on (a) SRC and ORC turbine power, and (b) cycle efficiency

can be checked in the rate of entropy generation by both cycles; as it is clear from Figure 10, the entropy generation increases with the rise in the engine speed (due to the increase in the heat transfer rate). as well as the entropy generation in the cycle, ORC is far less than the SRC cycle, so the exergy destruction rate of the ORC is lower than the SRC.

The following figure shows the effect of engine speed on exergy efficiency for the engine, ORC, and SRC cycles; The recovery cycles have led to an increase in the exergy efficiency of the engine for all operational revolutions per minute also the results show that the exergy efficiency increases with the rise of the engine speed. Exergy efficiency decreases after passing the engine speed range of 1500 to 1600 rpm. On the other hand, the results show that on average (for all rpms), the presence of ORC and SRC recovery cycles can lead to an increase in exergy efficiency by 8.85% and 8.25% (respectively). Also, the most significant increase in exergy efficiency due to heat recovery occurs at the lowest speed, at 600 rpm; the exergy efficiency can increase by 46.05% and 17.42% for the ORC and SRC, respectively, by adding the waste heat recovery cycle. This is also shown in Figure 11, and as it is clear from this diagram, the existence of the recovery cycle at low engine speed strongly affects the exergy efficiency. After passing through the low-speed area, the exergy efficiency increases due to the existence of the recovery cycle 7% in the best condition.

CSO cycle

Figure 12 shows the effect of engine speed on the output power and efficiency of the CSO cycle. As it is clear from the graph, with the increase in engine speed, the output power from CSO rises, and after passing 1600 rpm, the power produced by the CSO cycle decreases from the

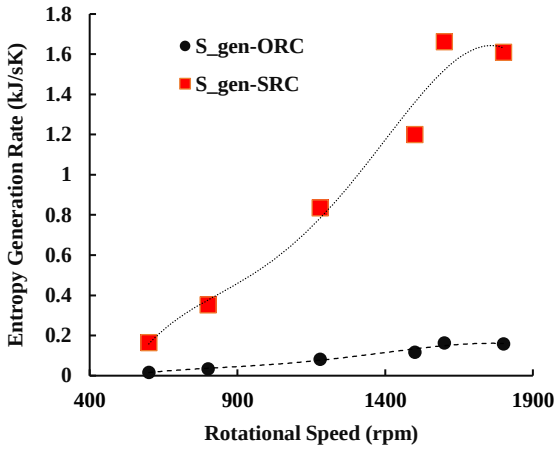

(a)

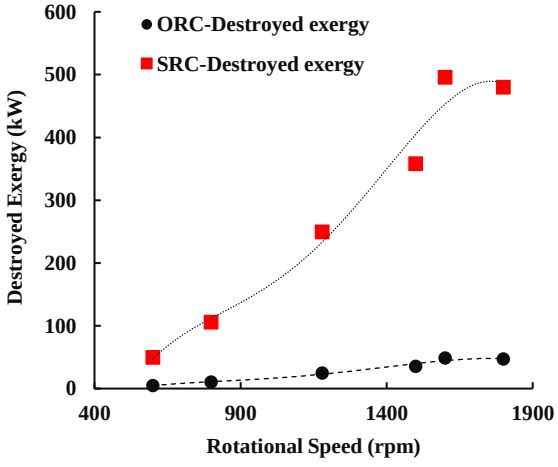

(b)

Figure 10. Effect of engine speed on (a) entropy generation, and (b) exergy destruction

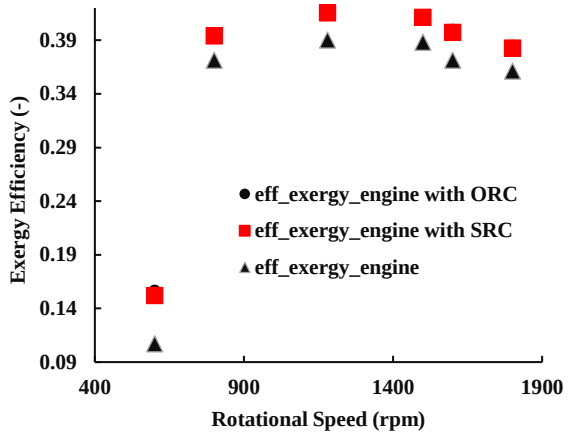

(a)

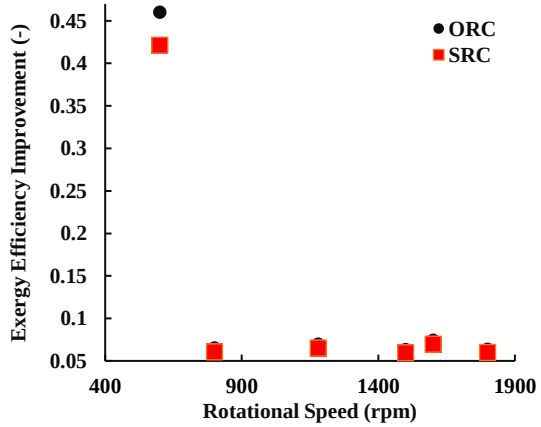

(b)

Figure 11. Effect of engine speed on (a) exergy efficiency, and (b) exergy efficiency improvement

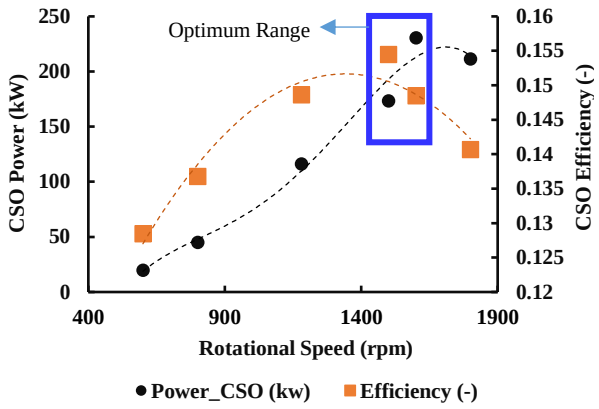

Figure 12. Effect of engine speed on CSO power and efficiency

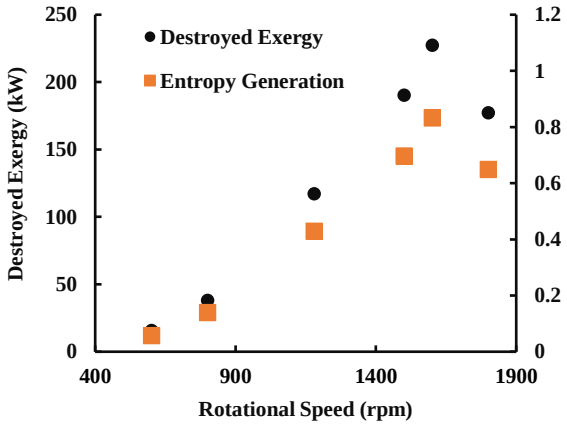

Figure 13. Effect of engine speed on destroyed exergy and entropy generation of CSO

engine's waste heat. On the other hand, the engine increases up to the range of 1500 rpm and drops after passing this point because the increase in the engine speed leads to a rise in the power up to a certain value, and after passing 1600 rpm, the rate of input energy to the cycle (from work produced by the recovery cycle) is increased compared to the output power, and as a result, the efficiency decreases. On the other hand, the important point is 1500 rpm, which can be introduced as the best performance point by considering energy efficiency. However, in terms of the power generation of the system, 1600 rpm produces more power, considering both power and efficiency perspectives, the range of 1500 to 1600 rpm can be introduced as the optimal performance range. In order to better study the power produced by the CSO cycle, the exergy destruction value of the cycle and the entropy generation should be investigated (Figure 13); In this regard, the following diagram shows the effect of engine speed on exergy destruction and entropy generation, increasing the engine speed up to 1600 rpm increases the rate of exergy destruction and entropy generation. However, after passing this speed, the rate of both parameters decreases.

Figures 14-a and 14-b show the effect of engine speed on engine exergy efficiency, CSO cycle, and also the amount of exergy improvement due to the use of CSO waste heat recovery system. The results of thermodynamic modeling show that for the CSO cycle, increasing the engine speed up to 1180 rpm leads to an increase in exergy efficiency, and from 1180 to 1500 rpm, the exergy efficiency remains relatively constant ((changes below) 1% efficiency). After passing 1500 rpm, the exergy efficiency decreases. On the other hand, the results show that the existence of a recovery cycle for the engine leads to an increase in exergy efficiency in all cycles, but the amount of increase in efficiency is different; the most tremendous increase in exergy efficiency is due to the use of CSO recovery cycle in the lowest engine speed (600 rpm) and is equivalent to 6% increase in exergy efficiency, on the other hand, the lowest increase in efficiency occurs at the highest engine speed (1800 rpm) and is equivalent to 3% increase in

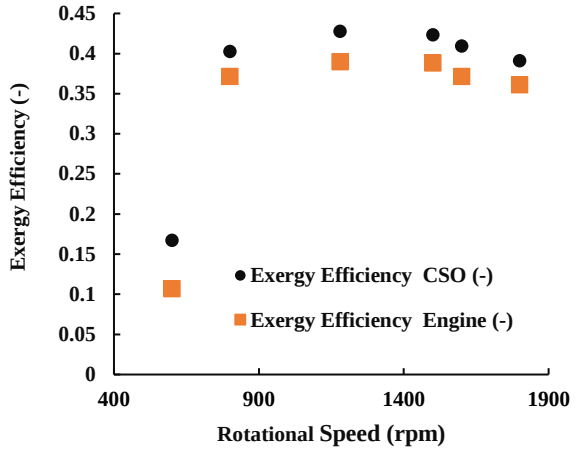

(a)

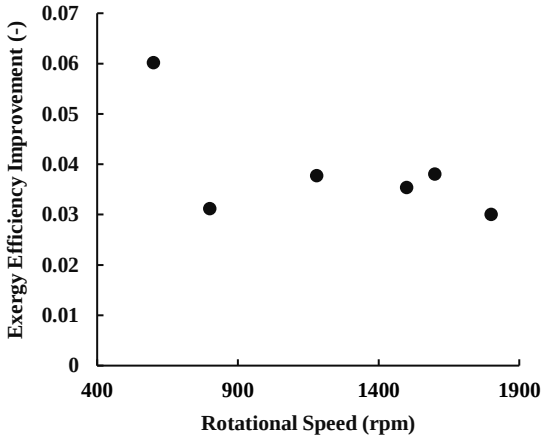

(b)

Figure 14. Effect of engine speed on destroyed exergy and entropy generation of CSO

exergy efficiency, also using the CSO waste heat recovery cycle has been able to increase the exergy efficiency by an average of 3.8%.

Overall comparison of ORC, SRC and CSO

In this section, the results obtained from the thermodynamic modeling of the waste heat recovery cycle are compared with each other to determine the optimal cycle in terms of performance. In this regard, in Figure 15, the effect of the engine speed on the total power by the engine and the recovery cycle has been shown separately for all three cycles. The results show that for all modes, the CSO cycle has a better performance compared to the rest of the cycles; on the other hand, it should be kept in mind that at low engine speeds (below 1000 rpm), the difference between the cycles is not obvious. However, by being in the optimal performance range (1500 to 1600 rpm), the performance of the CSO cycle is far better than the rest of the cycles, although, as shown, the ORC cycle after can perform better significantly. The CSO cycle can perform 37.72% better in the optimal range than the ORC cycle. Also, using the engine alone at the highest operating speed could produce power equal to 2540 kW. However, using the waste heat recovery cycle has increased this power by 8.3% and reached 2751 kW.

In Figure 16, the effect of engine speed on the efficiency of recovery cycles is shown; The results show that the use of ORC and SRC recovery cycles at different engine speeds does not have much effect on the efficiency, and the efficiency remains almost constant. However, the CSO cycle performs better than the other two cycles and can have more variations by being placed in different speeds. The system experiences a significant increase in efficiency at optimal engine speed.

In order to compare the improved system with the conventional systems, the FESR parameter can be used; as it is clear from the diagram, the system can be compared with the conventional electricity production

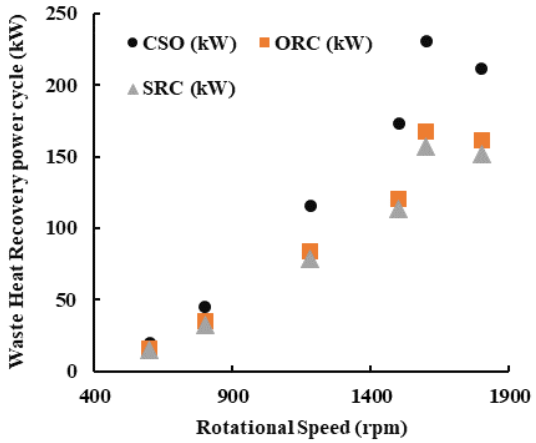

(a)

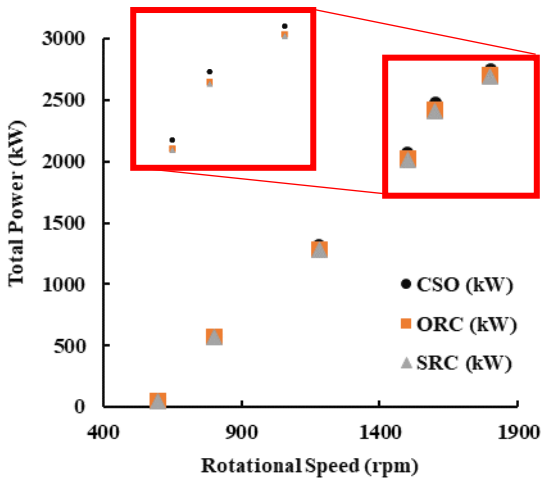

(b)

Figure 15. Effect of engine speed on (a) waste heat recovery power cycle, and (b) total power

systems for all conditions and the fuel energy saving ratio (FESR) of CSO cycle is higher than other heat recovery systems. Also the results showed that the system in the optimal range could be up to 33.9 % of FESR, also CSO cycle in this range has 3.5% more FESR compared to ORC cycle. The effect of engine speed on fuel energy saving ratio is shown in Figure 17.

Also, in the graph below, the effect of the engine speed on the exergy efficiency of the recovery cycles was compared, the system at the lowest speed has a low exergy efficiency, the efficiency increases with the rise of the engine speed and of course the heat produced by the engine. After crossing the optimal range of the system, the exergy efficiency decreases due to the reduction of the waste heat input to the cycles. it is also worth mentioning that from the exergy point of view CSO have better performance. Of course, the CSO cycle performance in the optimal performance range is larger than the other two cycles. The effect of engine speed on exergy efficiency is shown in Figure 18.

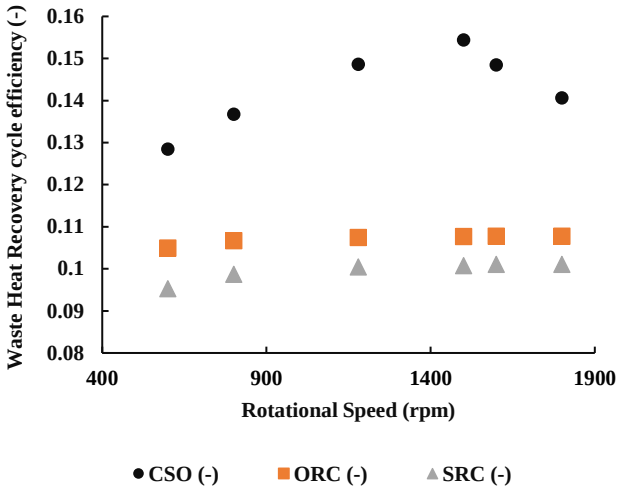

Figure 16. Effect of engine speed on waste heat recovery efficiencies

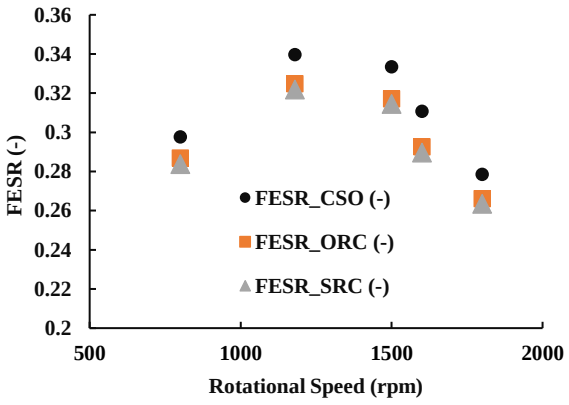

Figure 17. Effect of engine speed on fuel energy saving ratio

In Figure 19, the average and maximum values of efficiency from the energy, exergy and FESR point of view of are shown, as it is clear from the graphs, the recovery system with CSO cycle has a much higher energy efficiency (33.6% on average and 42.6% for the maximum mode) compared to the other two cycles, and the ORC and SRC cycles have similar values in terms of average and maximum efficiency. However, all cycles have similar exergy efficiency and FESR (whether maximum or average).

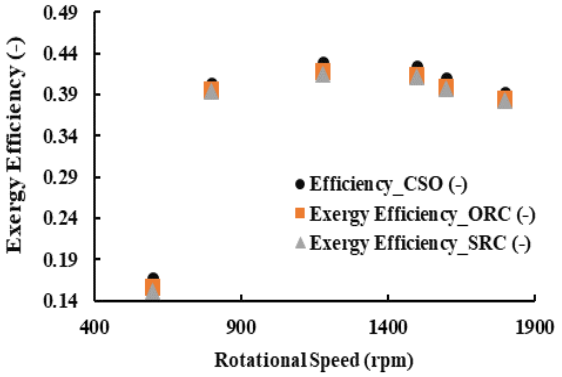

Figure 18. Effect of engine speed on exergy efficiency

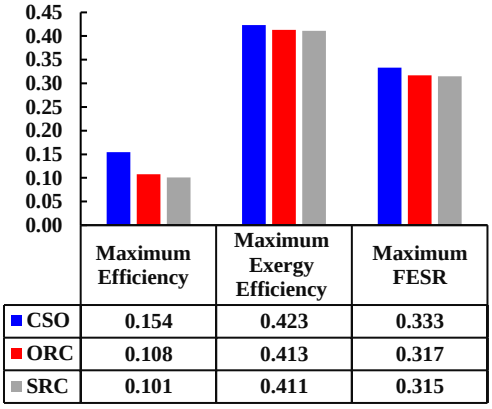

	Maximum Efficiency	Maximum Exergy Efficiency	Maximum FESR
CSO	0.154	0.423	0.333
ORC	0.108	0.413	0.317
SRC	0.101	0.411	0.315

(a)

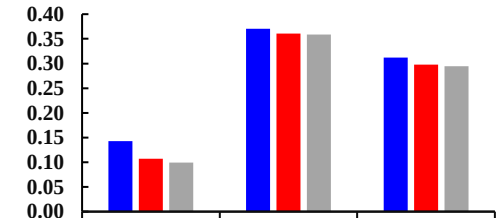

	Average Efficiency	Average Exergy Efficiency	Average FESR
CSO	0.143	0.370	0.312
ORC	0.107	0.361	0.297
SRC	0.100	0.359	0.295

(b)

Figure 19. (a) Maximum and (b) average performance comparison

Environmental analysis

In order to study the performance of the system from the environmental point of view, CO_2 production of the system has been compared to conventional methods. In Figure 20a, the effect of rotational speed on annual CO_2 reduction has been shown. As it can be seen from the figure by increasing the rotational speed, annual CO_2 reduction rises and the maximum CO_2 reduction is 845 tons per year. On the other hand, the reduction ratio has been shown in Figure 20b; the reduction ratio shows a nonlinear behavior and reaches a maximum valuof 1180 rpm. The best environmental performance belongs to CSO in comparison to ORC and SRC. The annual CO_2 reduction of CSO is 5.1% higher than SRC and 6.2% higher than ORC for best operating condition. On the other hand, CO_2 production causes tax paying. So by increasing the system's efficiency and making system more effective, the annual tax reduction can give an appropriate environmental approach. System's annual tax reduction rises by increasing the rotational speed for all waste heat recovery cycles (CSO, ORC and SRC). As it could be predictable the highest tax reduction belongs to CSO and the CSO can reduce the tax about $25351 peryear.

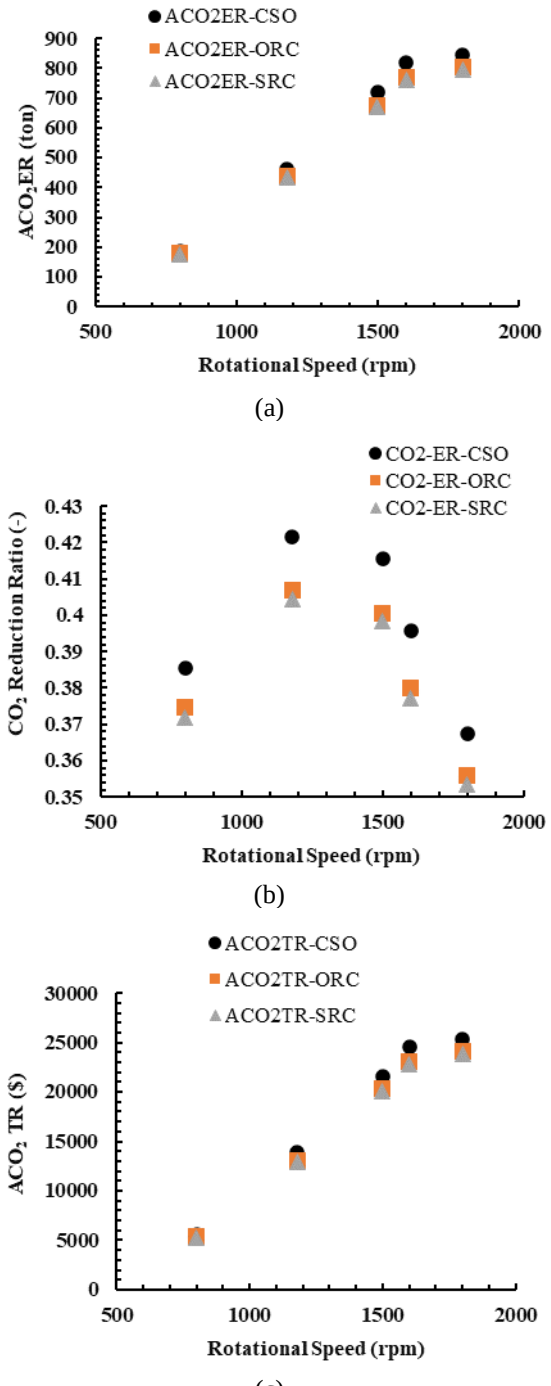

Figure 20. (a) Annual CO_2 emission reduction, (b) CO_2 reduction ratio and, (c) Annual CO_2 tax reduction

CONCLUSION

This research focused on the evaluation and investigation of waste heat generated by the MTU 4000 R43L engine through a series of experimental studies. Our findings, which encompassed considerations of critical constraints such as dew point and back pressure, led to the design and evaluation of three waste heat recovery cycles: Organic Rankine Cycle (ORC), Steam Rankine Cycle (SRC), and Combined Supercritical Organic Rankine Cycle (CSO). Our analysis encompassed multiple dimensions, including energy, exergy, economics, and environmental impact, yielding the following significant results:

1. *Optimal Engine Speed:* We observed a non-linear relationship between engine speed and waste heat. Increasing the speed up to 1600 rpm resulted in a corresponding increase in engine waste heat. Beyond this point, waste heat decreased. The system demonstrated its highest waste heat potential (1553 kW) at 1600 rpm, representing a promising opportunity for the recovery cycle.
2. *Energy Efficiency:* When comparing the cycles from an energy perspective, the CSO cycle consistently outperformed the ORC and SRC cycles. In the best-case scenario, the CSO cycle exhibited an efficiency that was 43.4% higher than the ORC cycle and 53.3% higher than the SRC cycle.
3. *Exergy Efficiency:* The CSO cycle also demonstrated superior exergy efficiency across all modes, albeit with a less significant difference compared to energy efficiency. In the best case, the CSO cycle's efficiency was 2.5% greater than that of the ORC cycle and 2.9% greater than the SRC cycle.
4. *Economic impact:* From an economic perspective, the CSO cycle proved to be the most cost-effective choice in all modes compared to the ORC and SRC

cycles. The maximum fuel savings achieved by the CSO, ORC, and SRC cycles were 33.3%, 31.7%, and 31.5%, respectively.

5. *Average performance metrics:* On average, the CSO cycle exhibited higher energy efficiency (14.3%), exergy efficiency (37.0%), and Fuel Economy and Sustainability Ratio (FESR) (31.2%) compared to the ORC and SRC cycles.
6. *Environmental benefits:* Our environmental assessment revealed that the CSO cycle offered the most favorable performance in terms of Annual CO2 Emission Reduction (ACO2ER), with a notable reduction in annual tax expenses by approximately $25,351 through the implementation of CSO waste heat recovery.

In conclusion, this research underscores the potential of waste heat recovery from the MTU 4000 R43L engine, with the CSO cycle emerging as the most efficient, cost-effective, and environmentally friendly option. These findings have significant implications for the utilization of waste heat in various industrial and energy applications, contributing to both economic savings and reduced environmental impact.

It could be a good suggestion to consider CHP and CCHP recovery cycles for future research and analyze the system from energy and exergy point of view.

REFERENCES

1. Seyfouri Z, Ameri M, Mehrabian MA. Energy, Exergy and Economic Analyses of Different Configurations for a Combined HGAX/ORC Cooling System. Iranian Journal of Science and Technology, Transactions of Mechanical Engineering. 2022;46(3):733-44. Doi: 10.1007/s40997-022-00497-x

2. Brands MC, Werner JR, Hoehne JL, Kramer S. Vehicle testing of Cummins turbocompound diesel engine. SAE Transactions. 1981:285-305. Available at: https://ntrs.nasa.gov/citations/19810005292

3. DiBella FA, DiNanno LR, Koplow MD. Laboratory and on-highway testing of diesel organic Rankine compound long-haul vehicle engine. SAE Technical Paper; 1983. Report No.: 0148-7191. Doi: 10.4271/830122

4. Endo T, Kawajiri S, Kojima Y, Takahashi K, Baba T, Ibaraki S, et al. Study on maximizing exergy in automotive engines. SAE Transactions. 2007:347-56. Available at: https://www.jstor.org/stable/44699283

5. He M, Zhang X, Zeng K, Gao K. A combined thermodynamic cycle used for waste heat recovery of internal combustion engine. Energy. 2011;36(12):6821-9. Doi: 10.1016/j.energy.2011.10.014

6. Shu G-Q, Yu G, Wei H, Liang X. Simulations of a bottoming organic rankine cycle (ORC) driven by waste heat in a diesel engine (DE). SAE Technical Paper; 2013. Report No.: 0148-7191. Doi: 10.4271/2013-01-0851

7. Jalili B, Ghafoori H, Jalili P. Investigation of carbon nano-tube (CNT) particles effect on the performance of a refrigeration cycle. International Journal of Material Science Innovations. 2014;2(1):8-17. Doi: 10.4271/2013-01-0851

8. Shu G, Yu G, Tian H, Wei H, Liang X, Huang Z. Multi-approach evaluations of a cascade-Organic Rankine Cycle (C-ORC) system driven by diesel engine waste heat: Part A–Thermodynamic evaluations. Energy conversion and management. 2016;108:579-95. Doi: 10.1016/j.enconman.2015.10.084

9. Lion S, Taccani R, Vlaskos I, Scrocco P, Vouvakos X, Kaiktsis L. Thermodynamic analysis of waste heat recovery using Organic Rankine Cycle (ORC) for a two-stroke low speed marine Diesel engine in IMO Tier II and Tier III operation. Energy. 2019;183:48-60. Doi: 10.1016/j.energy.2019.06.123

10. Mohammed AG, Mosleh M, El-Maghlany WM, Ammar NR. Performance analysis of supercritical ORC utilizing marine diesel engine waste heat recovery. Alexandria Engineering Journal. 2020;59(2):893-904. Doi: 10.1016/j.aej.2020.03.021

11. Boodaghi H, Etghani MM, Sedighi K. Performance analysis of a dual-loop bottoming organic Rankine cycle (ORC) for waste heat recovery of a heavy-duty diesel engine, Part I: Thermodynamic analysis. Energy Conversion and Management. 2021;241:113830. Doi: 10.1016/j.enconman.2021.113830

12. Neto RdO, Sotomonte CAR, Coronado CJR. Off-design model of an ORC system for waste heat recovery of an internal combustion engine. Applied Thermal Engineering. 2021;195:117188. Doi: 10.1016/j.applthermaleng.2021.117188

13. Ping X, Yang F, Zhang H, Zhang W, Zhang J, Song G, et al. Prediction and optimization of power output of single screw expander in organic Rankine cycle (ORC) for diesel engine waste heat recovery. Applied Thermal Engineering. 2021;182:116048. Doi: 10.1016/j.applthermaleng.2020.116048

14. LUO W, CHEN W, JIANG A, TIAN Z. Comparative Analysis of Thermodynamics Performances of ORC Systems Recovering Waste Heat from Ship Diesel Engines. China Mechanical Engineering. 2022;33(04):452. Available at: http://www.cmemo.org.cn/EN/abstract/abstract8727.shtml

15. Alizadeh Kharkeshi B, Shafaghat R, Mohebi M, Talesh Amiri S, Mehrabiyan M. Numerical simulation of a heavy-duty diesel engine to evaluate the effect of fuel injection duration on engine performance and emission. International Journal of Engineering. 2021;34(11):2442-51. Doi: 10.5829/IJE.2021.34.11B.08

16. Mayer A. Number-based emission limits, VERT-DPF-verification procedure and experience with 8000 retrofits. VERT, Switzerland. 2004. Doi: 10.1007/978-3-319-27276-4_34

17. Abbasi M, Chahartaghi M, Hashemian SM. Energy, exergy, and economic evaluations of a CCHP system by using the internal combustion engines and gas turbine as prime movers. Energy conversion and management. 2018;173:359-74. Doi: 10.1016/j.enconman.2018.07.095

18. Chahartaghi M, Kharkeshi BA. Performance analysis of a combined cooling, heating and power system with PEM fuel cell as a prime mover. Applied Thermal Engineering. 2018;128:805-17. Doi: 10.1016/j.applthermaleng.2017.09.072

19. Bejan A, Tsatsaronis G, Moran MJ. Thermal design and optimization: John Wiley & Sons; 1995.

20. Chahartaghi M, Alizadeh-Kharkeshi B. Performance analysis of a combined cooling, heating and power system driven by PEM fuel cell at different conditions. Modares Mechanical Engineering. 2016;16(3):383-94. [In Persian]

21. Sheykhi M, Chahartaghi M, Balakheli MM, Kharkeshi BA, Miri SM. Energy, exergy, environmental, and economic modeling of combined cooling, heating and power system with Stirling engine and absorption chiller. Energy Conversion and Management. 2019;180:183-95. Doi: 10.1016/j.enconman.2018.10.102

22. Kharkeshi BA, Mehregan M, Sheykhi M. Sensitivity analysis of energy, exergy, and environmental models for a combined cooling, heating, and power system at different operating conditions of proton exchange membrane fuel cell. Environmental Progress & Sustainable Energy. 2023. Doi: 10.5829/IJEE.2023.14.01.0

23. Sheykhi M, Chahartaghi M, Hashemian SM. Performance evaluation of a combined heat and power system with Stirling engine for residential applications. Iranian Journal of Science and Technology, Transactions of Mechanical Engineering. 2020;44(4):975-84. Doi: 10.1007/s40997-019-00303-1

Persian Abstract

چکیده

در این مقاله، یک موتور دیزل سنگین با استفاده از مطالعه تجربی و مدل‌سازی ترمودینامیکی برای بررسی اثر دور موتور بر گرمای هدر رفته مورد مطالعه قرار گرفت. سه چرخه ORC، SRC و CSO برای بازیابی گرمای تلف شده از اینترکولر، مبدل حرارتی آب و گاز خروجی معرفی شدند. نتایج نشان داد که افزایش سرعت تا ۱۶۰۰ دور در دقیقه منجر به افزایش گرمای اتلاف موتور می شود و پس از عبور از این سرعت، حرارت تلف شده کاهش می یابد و رفتار غیر خطی مشاهده می شود. از نقطه نظر انرژی، در بهترین شرایط، بازده چرخه CSO ۴۳/۴ درصد بیشتر از چرخه ORC و ۵۳/۳ درصد بیشتر از چرخه SRC است. با این حال، تفاوت بین سه چرخه معرفی شده از نقطه نظر اکسرژی ناچیز است. نتایج نسبت صرفه جویی در انرژی سوخت نشان داد که چرخه CSO نسبت به چرخه های ORC و SRC برای همه حالت ها اقتصادی تر است. CSO بالاترین عملکرد را در ACO2ER دارد و نرخ ACO2ER CSO بالاترین است، همچنین استفاده از بازیابی حرارت اتلاف CSO می تواند مالیات سالانه را حدود ۲۵۳۵۱ دلار در سال کاهش دهد.